Superconductor Science and Technology

Magnetic relaxation induced by transverse flux shaking in MgB_2 superconductors

To cite this article: J Luzuriaga *et al* 2008 *Supercond. Sci. Technol.* **22** 015021

Supercond. Sci. Technol. **22** (2009) 015021 (6pp) doi:10.1088/0953-2048/22/1/015021

Magnetic relaxation induced by transverse flux shaking in MgB_2 superconductors

J Luzuriaga[1], A Badía-Majós[2], G Nieva[1], J L Giordano[3], C López[4], A Serquis[1] and G Serrano[1]

[1] Centro Atómico Bariloche, CNEA, Instituto Balseiro, UNC, Argentina
[2] Departamento de Física de la Materia Condensada–ICMA, Universidad de Zaragoza–CSIC, Spain
[3] Departamento de Ciencias de la Ingeniería, Universidad de Talca, Chile
[4] Departamento de Matemáticas, Universidad de Alcalá de Henares, Spain

E-mail: luzuriag@cab.cnea.gov.ar

Received 1 August 2008, in final form 14 October 2008
Published 10 December 2008
Online at stacks.iop.org/SUST/22/015021

Abstract

We report on measurements and numerical simulations of the behavior of MgB_2 superconductors when magnetic field components are applied along mutually perpendicular directions. By closely matching the geometry in simulations and measurements, full quantitative agreement is found. The critical state theory and a single phenomenological law, i.e. the field dependence of the critical current density $J_c(B)$, are sufficient for a full quantitative description of the measurements. These were performed in thick strips of carbon nanotube doped MgB_2 samples. Magnetization was measured in two orthogonal directions using a SQUID magnetometer. Magnetic relaxation effects induced by the application of an oscillatory perpendicular field were observed and simulated numerically. The measurements confirm the numerical predictions, that two relaxation regimes appear, depending on the amplitude of the applied magnetic field. The overall agreement constitutes a convincing validation of the critical state model and the numerical procedures used.

(Some figures in this article are in colour only in the electronic version)

1. Introduction

Magnetic relaxation effects induced by the application of a transverse ac field have recently been reported in high-T_c superconducting samples [1, 2]. Researchers have taken advantage of this phenomenon for getting rid of unwanted irreversible components of the sample's magnetic moment $\mathbf{M}_{irr}$ [1]. We recall that $\mathbf{M}_{irr}$ relates to the existence of gradients in the flux density, caused by the pinning of vortices in the mixed state.

To be specific, when applying an oscillating ac field perpendicular to the vector $\mathbf{M}_{irr}$ one may delete any trace of this quantity and just record a *distilled* reversible magnetization $\mathbf{M}_{rev}$, which is basically untouched by the process. In brief, as the irreversible shielding capacity of the sample is bounded (J_c), when the external excitation requires a new component of $\mathbf{J}$ the original current distribution changes and the related magnetic moment diminishes or even vanishes.

From the theoretical point of view, the critical state theory seems to capture the essential physics behind the experimental facts. Of special note are the so-called shaking effects on the flux lines. They have been predicted either for thin strips within a purely analytical approach [3, 4] or for arbitrary section strips in numerical studies [5]. In both cases, the Lorentz force related critical current density $J_{c\perp}$ (here $\perp$ is relative to the local magnetic induction) is the basic concept behind the predictions of the sample's magnetic response. Remarkably, the component of $\mathbf{M}_{irr}$ perpendicular to the oscillating magnetic field relaxes in the complete absence of thermal activation effects. On the other hand, it was predicted [5] that relaxation may essentially stop in some metastable state or quickly lead to $\mathbf{M}_{rev}$, depending on the actual experimental conditions.

To our knowledge there is no experimental work on the residual critical state along the oscillating field and the question about the predicted complete/incomplete relaxation in terms of the amplitude of the applied magnetic field [5] also remains to be answered experimentally.

This work was devoted to investigating the shaking effect on both components of $\mathbf{M}$ for MgB_2 samples. It is, as far as we

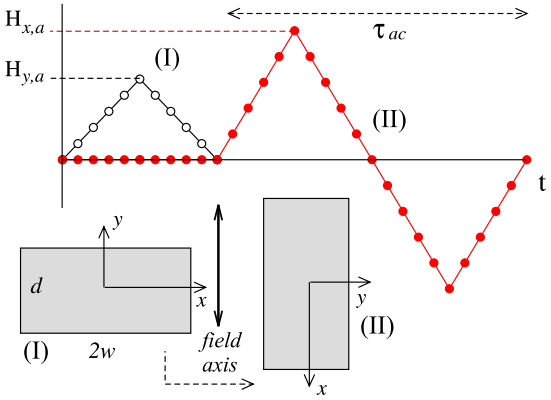

Figure 1. Detail of the experiment. First, the field is applied along the sample y-axis, and removed (I). Then the sample is rotated by 90° and field cycles are performed with the field applied along the sample x-axis (II). The magnetic moment is measured along the X and Y axes during the cycle.

know, the first report of such effects in this superconductor. The practical absence of anisotropy and the high pinning forces make the material a natural candidate for measuring the connection between the phenomenological critical state approach and flux shaking effects. We have matched the geometry of the measured sample and the simulations, and also paid particular attention to the magnetic field dependence of the critical current. In this way all the parameters which enter into the calculation are fixed, and we are therefore able to test the validity of the approximations. The results show full agreement between the theoretical prediction and experiments at a quantitative level. A single phenomenological relation $J_{c\perp}(B)$, i.e. the perpendicular (field dependent) critical current density, has been used. Such a quantity is obtained from a detailed analysis of the one-dimensional $M(H)$ response [6]. This gives confidence in the general applicability of the model, and proves that the essential physics is captured by the critical state approach [5].

2. Experimental details

The experiments were carried out on a polycrystalline MgB_2 sample doped with a 10 at.% concentration of single walled carbon nanotubes (SWCNT). A T_c of ∼36 K was obtained from the onset of the superconducting transition in a magnetization measurement. As has been shown elsewhere [7], the SWCNT increase the pinning force, and therefore the critical current. Sample dimensions were 0.31 × 0.66 × 3.0 mm. The longest dimension (3 mm) was set parallel to the rotation axis used for establishing the crossed field configuration (see figure 1). The smallest dimension, (0.31 mm), is matched with the y-axis (d), and the remaining (0.66 mm) with the x-axis ($2w$). The sample size along the z-axis cannot be increased due to the space available within the magnetometer. Nevertheless, the actual aspect ratio of the sample has allowed a suitable quantitative analysis within the long strip approximation.

We have used a custom built probe [8] with a rotating sample holder inside a Quantum Design SQUID magnetometer. Rotation around a horizontal axis, perpendicular to the magnetic field direction, is allowed. The sample holder consists of a nylon cylindrical rotating cradle of diameter 3 mm which can turn on an axis perpendicular to the magnetic field of the magnetometer. On top of the sample holder a stepper motor moves the cradle by means of a loop of Manganin wire which provides the mechanical linkage. There is some slippage in this connection, so we checked the alignment of the sample, with an estimated error of about 1°, by measuring the perpendicular and parallel components of the remanent magnetization of the sample after rotation. The alignment before rotation is visually checked before each run, before lowering the sample. The background signal of the holder, measured above the superconducting transition of the sample, is a few per cent of the sample signal and is taken into account when analyzing the data.

The crossed field configuration (see figure 1) was achieved experimentally by placing the sample so that the y-axis was parallel to the axis of the magnetic field. Then it was cooled in this position down to 10 K in zero field. Subsequently, a magnetic field H_y was applied and then removed, producing a remanent magnetic moment along the y-axis. With no magnetic field present in the magnet so as to avoid magnetic induction effects, the sample was rotated by 90° in order to place the x-axis parallel to the field direction. Following this, H_x was cycled several times. The values of τ_{ac} varied between 66 and 120 min from the smallest to the largest $H_{x,a}$ (maximum field reached during a cycle).

Taking advantage of the SQUID's capability to simultaneously record the longitudinal and transverse components of magnetization with respect to the field, we measured the vector $(M_x(t), M_y(t))$ while oscillating the applied field H_x. All the experiments reported were performed at 10 K. We have checked that at this temperatures flux creep effects are negligible, i.e. $\Delta M/M < 0.01$ in a typical measurement period of 5 h.

The inductive quantity shown in this work corresponds to the sample's magnetic moment per unit volume (i.e. the magnetization): $\mu_0 M = (4\pi/10) \times (m/v)$ in millitesla, where m is the measured magnetic moment in erg G^{-1} (emu) from the SQUID output, and v is the specimen volume in cubic centimeters. The applied magnetic strength H is expressed in terms of the magnetic induction $B = \mu_0 H$ in a vacuum. As usual, this relates to the approximation that the reversible magnetic response of the sample may be neglected as compared to the irreversible contribution, i.e. the magnetic moment related to the pinning induced flux density gradients.

3. Experimental and numerical results

3.1. Analysis of the experimental data

In figure 2 we show the magnetization in both orthogonal directions as the field along the x-axis is swept through several cycles. We have plotted M_x and M_y against the applied field H_x. In fact the position in the magnetic field cycle is the relevant parameter because we are in the steady state in terms of the current distribution. Experimental time scales are long compared with transients associated with flux

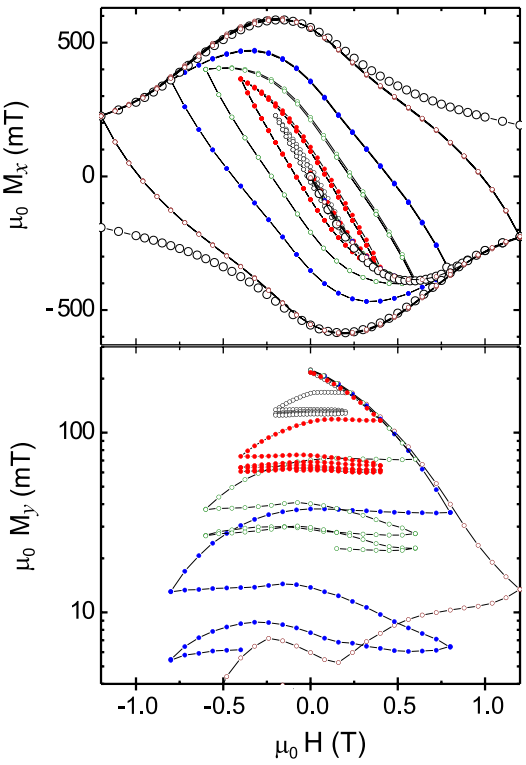

Figure 2. Experimental results for $\mu_0 H_{y,a} = 0.4$ T. In the lower panel we show M_y as a function of magnetic field; the upper panel shows equivalent plots of M_x. The curves correspond to the following values of the maximum field reached in the sweep along the x-axis: $\mu_0 H_{x,a} = 0.2$, 0.4, 0.6, 0.8 and 1.2 T. The larger circles in the M_x versus H_x plot correspond to an extended magnetization loop with $\mu_0 H_{\max} = 3$ T.

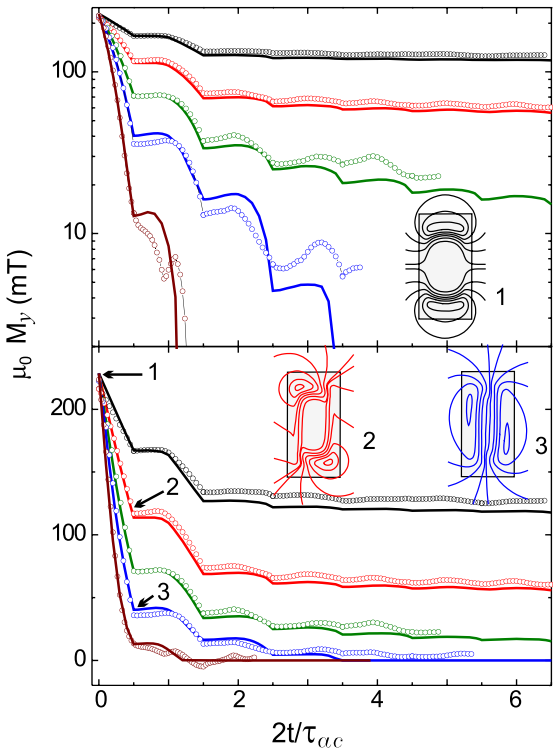

Figure 3. Plots of $M_y(t)$ against time both in logarithmic and linear scales: symbols are for measurements and full lines for the model. Notice the two regimes: for $H < H_{px}$ a finite magnetization remains, for $H > H_{px}$ the magnetization collapses to zero. The curves from top to bottom correspond to $\mu_0 H_{x,a} = 0.2$, 0.4, 0.6, 0.8 and 1.2 T. The insets show the magnetic flux lines penetrating the sample: (1) just after inducing the remanent state for $\mu_0 H_{y,a} = 0.4$ T and rotating the sample, (2) subsequent to the first half-cycle of H_x for an amplitude $\mu_0 H_{x,a} = 0.4$ T and (3) the same for $\mu_0 H_{x,a} = 0.8$ T.

changes and small with regard to flux creep. In other words, one may assume that the sample's internal flux distribution instantaneously follows the applied excitation, whereas it keeps stationary until new variations are performed. The initial field amplitude for the trapped magnetic field was $\mu_0 H_{y,a} = 0.4$ T while $H_{x,a}$ was swept up to maximum values $\mu_0 H_{x,a} = 0.2$, 0.4, 0.6, 0.8 and 1.2 T.

The behavior observed is very similar to the calculations reported in figure 7 of the paper by Badía and López [5], who performed simulations using the same sample shape. M_y data are shown in figure 3 as a function of time t (expressed in units of the ac field periodicity $\tau_{\rm ac}$). Two relaxation regimes are visible, as predicted in [5], depending on the amplitude of the cycling field $H_{x,a}$. When $H_{x,a}$ is lower than the penetration field along the x-axis, H_{px}, the magnetization M_y essentially evolves towards a finite steady state value after several cycles with a small periodic component due to the redistribution of critical currents produced by $H_x(t)$. For higher fields $H_{x,a} > H_{px}$ the magnetization M_y quickly collapses to zero, as can be seen in the lower curves of figure 3.

The full penetration field H_{px} may be estimated from the constant $J_{\rm c}$ approximation in [9] as $H_{px} = 0.85 w J_{\rm c0}/2$. In our case, this gives 0.84 T. Recalling that this quantity relates to the disappearance of the flux free core within the sample, we have refined this value to 0.76 T when the actual $J_{\rm c}(B)$ is taken into account. A rather accurate determination can be made based on the plot of the core's area in terms of the applied field. On the other hand, as one can check from the experimental data of figure 2, this agrees approximately with the criterion often used empirically of the intersection between initial magnetization and the hysteresis cycle.

Other details of the theory are also reproduced: in particular, we observe a step-like descent of M_y with plateaus when the absolute value of the field H_x decreases, i.e. after a maximum or a minimum of H_x. Nevertheless, the full description of our experimental observations required some refinement of the theory.

To start with, the magnetization process simulated in [5] consisted of preparing an initial diamagnetic state in M_y and subsequently applying the transverse field oscillations. Owing to the experimental constraints in this work, the starting point was a remanent paramagnetic moment M_y produced by first increasing H_y, then putting it back to zero, and eventually cycling the transverse field H_x. Up to a point this is a mirror image of [5], with field leaking out of the sample instead of drifting in. Although the initial M_y state does not modify the qualitative properties of the further relaxation, the full quantitative prediction (transients included) requires the simulation of the exact process. On the other hand, we found that accounting for a proper magnetic field dependence of $J_{\rm c\perp}$

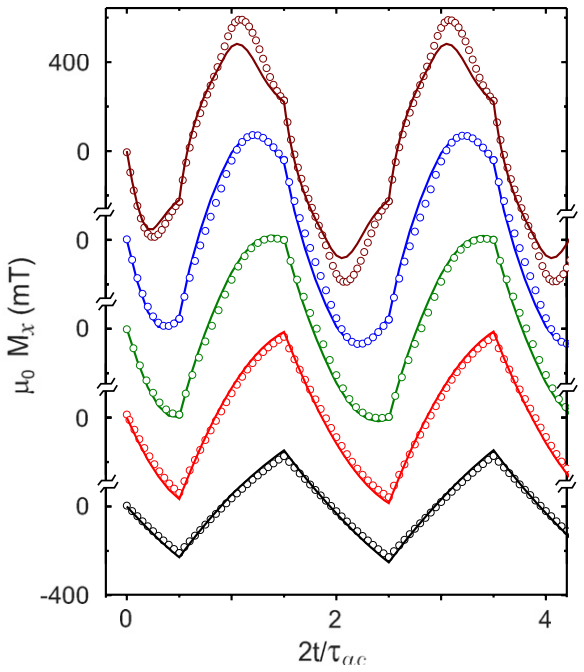

Figure 4. Magnetization along the x-axis $M_x(t)$ as a function of time: symbols are for measurements and full lines for the model. The curves correspond to $\mu_0 H_{x,a} = 0.2$, 0.4, 0.6, 0.8 and 1.2 T. For higher values of H_x the response of M_x also shows a greater amplitude.

is much more crucial. Consequently, although relying on the same physical principles and similar numerical methods, we have performed new simulations for this work.

In figure 3 we show measurements of M_y as a function of time compared with the results of the simulations, in both linear and logarithmic scales. In these graphs one can observe the tendency of M_y to a finite saturation value for low values of the amplitude $H_{x,a}$ and its rapid collapse to zero for values of $H_{x,a}$ above the penetration field H_{px}. The excellent agreement between the simulations and the measurements can be clearly seen. It should be remarked that the measurement of low values of M_y is subject to larger experimental errors due to some unshielded induction of the oscillating field along the x-axis. This is apparent in particular in the logarithmic plots, where the small discrepancies are enlarged by the scale. The errors arise because small imperfections in the cylindrical symmetry of the probe cause the sample to be slightly off center with respect to the set of perpendicular pickup coils, producing cross-talk between their signals. We compensate for this by using the standard procedure indicated by the magnetometer's manufacturer, but the errors increase when the difference between both signals is larger (i.e. small remanent M_y and large oscillating M_x).

In figure 4 we show the measurements of M_x which follow the cycle imposed by the field, together with the corresponding numerical results, also showing quantitative agreement. The magnetization along x is cyclic after the first complete cycle in H_x. It should be noticed that M_x is always in a metastable state during the cycle so that the sample as a whole is not in thermodynamic equilibrium, even when the value of M_y is close to zero (or to the reversible equilibrium value). In experiments such as those of Beidenkopf *et al* [10], which use perpendicular fields and aim at measuring a thermodynamic state, this fact could perhaps be relevant, especially if the dimension d cannot be neglected.

As a final experimental issue, we stress that the quantitative analysis of the sample's response $(M_x(t), M_y(t))$ has required a careful determination of the critical current density dependence $J_{c\perp}(B)$. In particular, we were interested in the low field region, and recall that problems arise when extracting $J_{c\perp}(B)$ from the width of the hysteresis loops $\Delta M(H)$ [11]. Thus, following [11], we prepared for this purpose a sample shaped as a thin disk from the same batch of material. From ΔM obtained by measuring with the magnetic field along the axis of the disk, we estimated a zero field critical current $J_{c0} = 6.0 \times 10^5$ A cm^{-2} which is in agreement with other measurements in this compound [7]. From the same magnetization loop we found that for fields below 3 T one can use the following fit:

$$J_{c\perp}(B) = \frac{J_{c0}}{(1 + B/B_0)^2} \tag{1}$$

with $B_0 = 1.25$ T. We emphasize that the above empirical expression was introduced for instrumental purposes as a very good description within our experimental range. In fact it can conveniently replace what one needs in a calculation, i.e. an interpolated table of $J_{c\perp}(B)$ data that come from a specific experiment.

3.2. Theoretical modeling

We recall that highly accurate predictions of the macroscopic response of type-II superconducting samples, i.e. average magnetic moment versus applied magnetic field, are typically made in terms of the usual critical state theory [6]. In this approach, the equilibrium configurations of flux quanta are treated by the macroscopic relation $|\mathbf{J} \times \mathbf{B}| \leqslant F_p$ between the volume pinning force and the average values of the current density and magnetic flux density. Thus, a maximum value for the pinning force is equivalent to a critical value in the component of the current density, perpendicular to the local magnetic induction ($J_\perp \leqslant J_{c,\perp}$). As regards the dynamical properties, and corresponding to a large dissipation when flux is eventually unpinned, one may treat the response of the sample by the Maxwell equations for the average fields, plus the condition $J_\perp = J_{c,\perp}$ in a magnetoquasistationary approach. In physical terms, the dissipation related time constant may be neglected, and evolution is controlled by the external excitation process through Ampère's and Faraday's laws. These concepts have been thoroughly discussed in some papers, deriving from our interpretation of the critical state in [12].

The actual application of the above ideas to flux shaking experiments for non-idealized geometries is not simple, and has been done either under ad hoc simplifying hypotheses for extreme geometries [3, 4] or by using numerical minimization techniques [5]. In our case, variational solutions of Faraday's law when the sample undergoes a magnetic process as shown in figure 1 have been obtained under the mutual inductance

approach (equation (2) in [5]). Let us give some details about how such a formulation arises.

In general, our three-dimensional proposal starts with the variational statement of the critical state [12]:

$$\texttt{Minimize} \quad \mathcal{C} \equiv \frac{\mu_0}{2}\int_{\mathbb{R}^3} |\vec{H}_{n+1} - \vec{H}_n|^2, \qquad \vec{J}_{n+1} \in \Delta \quad (2)$$

with $\vec{H}_n$ the magnetic field at the time layer n and the restriction $\vec{J}_{n+1} \in \Delta$ applied to the volume of the superconductor, i.e. the current density vector is restricted to belong to some subset Δ. In the case of long samples (the situation stated in this work) the latter condition may be expressed in the aforementioned form $J_\perp \leqslant J_{c,\perp}$ because the direction of $\vec{J}$ is determined by symmetry (z-axis in our sample).

Physically, induced supercurrents will be such that the magnetic field configuration over the whole space keeps as close as possible to the previous time layer (as a consequence of Faraday's law). One can show that this is achieved by the condition that $\vec{J}$ belongs to the boundary of the allowed region, i.e. $J_\perp = J_{c,\perp}$ in the current case.

From a more technical point of view, in order to get rid of the mathematical difficulties introduced by dealing with $\mathbb{R}^3$, and taking advantage of classical electrodynamics manipulations, one can show that the principle may be restated in terms of the current density and vector potential as follows:

$$\begin{aligned}\texttt{Minimize} \quad & \mathcal{F} \\ & \equiv \int_\Omega\int_\Omega \left[\frac{\vec{J}_{n+1}(\vec{x})\cdot\vec{J}_{n+1}(\vec{x}\,')}{|\vec{x}-\vec{x}\,'|} - 2\frac{\vec{J}_n(\vec{x})\cdot\vec{J}_{n+1}(\vec{x}\,')}{|\vec{x}-\vec{x}\,'|}\right] \\ & + \frac{8\pi}{\mu_0}\int_\Omega \left(\vec{A}_{e,n+1} - \vec{A}_{e,n}\right)\cdot\vec{J}_{n+1} \qquad (3)\end{aligned}$$

for $\vec{J}_{n+1} \in \Delta$, with Ω, the superconducting volume, and $\vec{A}_e$ the applied vector potential.

On the other hand, notice that in our problem (assuming the long sample approximation), the current density may be thought as a stack of parallel wires along the z-axis, each with a current flow $\pm I_c$ (or 0), where $I_c = J_c s$ and s is the cross sectional area of the wire. Then, the variational statement may be discretized by means of the mutual inductance picture. One is just led to minimize the function

$$\begin{aligned}\mathrm{F}[\{I_i\}] \equiv & \tfrac{1}{2}\sum_{i,j} I_{i,n+1} M_{ij} I_{j,n+1} - \sum_{i,j} I_{\mathrm{i,n}} M_{ij} I_{j,n+1} \\ & + \mu_0 \sum_i I_{i,n+1}(A_{e,n+1} - A_{e,n}), \qquad (4)\end{aligned}$$

with $\{I_i\}$ the unknown set of electrical current values at the chosen collection of circuits, A_e the applied vector potential and M_{ij} the mutual inductance matrix. These coefficients are the geometrical property connecting two circuits given by the Neumann formula which one can easily recover when obtaining equation (3) from equation (4), i.e.

$$\frac{\mu_0}{4\pi}\int_\Omega\int_\Omega \frac{\vec{J}(\vec{x})\cdot\vec{J}(\vec{x}\,')}{|\vec{x}-\vec{x}\,'|}\,\mathrm{d}^3\,\vec{x}\,\mathrm{d}^3\vec{x}\,' \equiv \sum_{i,j} I_i M_{ij} I_j. \qquad (5)$$

Finally, recall that the minimization of $\mathrm{F}[\{I_i\}]$ in equation (4) is constrained by the current restriction $I_i \leqslant I_c \;\forall\, i$.

For the current work, a local field dependence of the critical current $I_{c,i}(B_i)$ has been used. Such refinement was needed for a more realistic approach to the experimental facts. As explained above, $J_{c,\perp}(B)$ was derived from a specifically designed experiment. Thus, the minimization has to be done in a self-consistent fashion, i.e. one solves the problem for the $(n+1)$th layer of time, by using $I_{c,i}(B_{n,i})$, then calculates $I_c(B_{n+1,i})$ again in terms of the new flux redistribution and iterates until convergence.

4. Discussion

The results of our calculations are shown in figures 3 and 4, in which the comparison between theory and experiment is displayed. The general trends are those described in [5], i.e. the remanent magnetization along the y-axis relaxes by means of the *ac* oscillation of $H_x(t)$. Two relaxation regimes may be observed, depending on the amplitude of the transverse field $H_{x,a}$. If this quantity is below the x-axis penetration field H_{px}, relaxation is slow. For a small number of ac cycles incomplete relaxation is observed. When this threshold is exceeded, relaxation is fast and the equilibrium magnetization is rapidly observed. Finally, the relaxation process takes place in a step-like descent, modulated by the ac cycle. On the other hand, some peculiarities have been noticed in the experiment that may be clearly ascribed to the field dependence of the critical current. To be specific, small bumps are visible in the step-descent of M_y that cannot be obtained from the field independent $J_{c\perp}$ approximation. Additionally, in the present case, the $M_x(t)$ response does not show a field independence (plateau) in part of the cycle as happens when $J_{c\perp}$ is field independent and $H_x > H_{px}$ [5, 6].

In conclusion, transverse flux experiments in MgB_2 samples have revealed a number of features that provide new insights into the problem of applying mutually perpendicular field components to type-II superconductors.

It has been shown that the behavior of the sample's magnetization along mutually perpendicular axes (M_x, M_y) is quantitatively reproduced by the critical state equations at a temperature of 10 K, and for an applied magnetic field in the range $0 < \mu_0 H < 1.2$ T. Basically, the theoretical model presented in [5] may be applied to this case.

In the present paper we have restricted ourselves to a situation where induced currents are mainly perpendicular to the field direction. Then, the condition $J_\perp \leqslant J_{c\perp}$ is equivalent to $J \leqslant J_c$, i.e. one may just focus on the modulus of the current density vector. More general cases will be addressed in future work.

On the other hand, a careful determination of the $J_{c\perp}(B)$ law has been required in order to achieve agreement between theory and experiment, both for $M_x(t)$ and $M_y(t)$. This observation completes recent work on YBCO samples [2], in which the field dependence of $J_{c\perp}$ was merely connected to a faster decay of M_y.

Acknowledgments

This work was partially supported by Chilean **FONDECyT** Project 1040668, Argentina **ANPCyT** PICT00-03-08937 and

UNCuyo 06/C252, and Spanish **CICyT** Projects MTM2006-10531 and MAT2005-06279-C03-01. JLG was partially supported by the Bicentennial Program in Science and Technology (PBCT) Grant ACT26, University of Talca (Chile), and the RAICES Program (SECyT Argentina), while on sabbatical leave at CAB.

References

[1] Willemin M, Rossel C, Hofer J, Keller H, Erb A and Walker E 1998 *Phys. Rev.* B **58** R5940
Willemin M, Schilling A, Keller H, Rossel C, Hofer J, Welp U, Kwok W K, Olson R J and Crabtree G W 1998 *Phys. Rev. Lett.* **81** 4236
[2] Vanderbemden Ph, Hong Z, Coombs T A, Denis S, Ausloos M, Schwartz J, Rutel I B, Babu N H, Cardwell D A and Campbell A M 2007 *Phys. Rev.* B **75** 174515
[3] Brandt E H and Mikitik G P 2002 *Phys. Rev. Lett.* **89** 027002
[4] Mikitik G P and Brandt E H 2003 *Phys. Rev.* B **67** 104511
[5] Badía A and López C 2007 *Phys. Rev.* B **76** 054504
[6] Bean C P 1964 *Rev. Mod. Phys.* **36** 31
[7] Serrano G, Serquis A, Dou S X, Soltanian S, Civale L, Maiorov B, Balakirev F and Jaime M 2008 *J. Appl. Phys.* **103** 023907
[8] Casa D 1995 *Thesis for 'Licenciado' degree* unpublished
[9] Brandt E H 1996 *Phys. Rev.* B **54** 4246
[10] Beidenkopf H, Avraham A, Myasoedov Y, Shtrikman H, Zeldov E, Rosenstein B, Brandt E H and Tamegai T 2005 *Phys. Rev. Lett.* **95** 257004
[11] Sanchez A and Navau C 2001 *Supercond. Sci. Technol.* **14** 444
[12] Badía A and López C 2001 *Phys. Rev. Lett.* **87** 127004